

Article

Clay Minerals and Element Geochemistry of Clastic Reservoirs in the Xiaganchaigou Formation of the Lenghuqi Area, Northern Qaidam Basin, China

Guoqiang Sun ^{1,2,*} , Yetong Wang ^{1,3}, Jiajia Guo ⁴, Meng Wang ^{1,3}, Yun Jiang ^{1,3} and Shile Pan ^{1,3}

¹ Northwest Institute of Eco-Environment and Resources, Chinese Academy of Sciences, Lanzhou 730000, China; wangyetong16@mails.ucas.edu.cn (Y.W.); wangmeng17@mails.ucas.ac.cn (M.W.); jiangyun1234554321@163.com (Y.J.); shilepan@163.com (S.P.)

² Key Laboratory of Petroleum Resources, Lanzhou 730000, China

³ University of Chinese Academy of Sciences, Beijing 100049, China

⁴ Research Institute of Petroleum Exploration and Development-Northwest, Petrochina, Lanzhou 730020, China; guojiajia123@petrochina.com.cn

* Correspondence: sguoqiang@lzb.ac.cn; Tel.: +86-0931-496-0858

Received: 17 October 2019; Accepted: 31 October 2019; Published: 3 November 2019



Abstract: We performed mineralogical and geochemical analyses of core samples from the Lenghuqi area in the northern marginal tectonic belt of the Qaidam Basin. The clay mineralogy of the Xiaganchaigou Formation sandstone is dominated by I + I/S + C types and characterized by high illite, a higher mixed-layer illite/smectite and chlorite, lesser smectite, and an absence of kaolinite. The clay minerals reflect that the Oligocene sedimentary basin formed in an arid-semi-arid climate with weak leaching and chemical weathering, and that diagenesis occurred in a K⁺- and Mg²⁺-rich alkaline environment. Measured major oxide concentrations show clear correlations. The lower Xiaganchaigou Formation is representative of a dry and cold freshwater sedimentary environment, whereas the upper Xiaganchaigou Formation is warmer and more humid. Trace element and rare earth element variations indicate that the paleoclimate conditions of the lower Xiaganchaigou Formation sedimentary period were relatively cold and dry, while the upper Xiaganchaigou Formation formed under warmer and more humid climate conditions. These findings reflect a global climate of a cold and dry period from the late Eocene to early Oligocene, and a short warming period in the late Oligocene.

Keywords: clay minerals; major elements; trace elements; sedimentary environment; diagenetic Environment; Qaidam Basin

1. Introduction

Clay minerals are widely distributed in sediments and are the products of sedimentation and diagenesis under certain conditions related to climate, water media, and provenance, which have important implications for interpreting the paleoenvironment, climate, and diagenesis processes. The study of clay mineralogy therefore provides important information regarding the characteristics of provenance, paleoclimate, and sedimentary and diagenetic environments, which shed insight on the sedimentary-diagenesis process [1–4]. The volatile elemental contents within sediments are commonly studied to extract information regarding environmental evolution. Particular environmental conditions influence the behavior of various elements differently during decomposition and migration, which affects their enrichment in different environments. Changes in element contents within sediments therefore often reflect a change in the environmental conditions during deposition [5–8]. Common major oxides (CaO, MgO, K₂O, Na₂O, SiO₂, Al₂O₃, Fe₂O₃, and TiO₂) [9,10] and trace elements (Sr, Ba, Ti, Fe, P, Mn, U, V, and Ni) [11,12] are sensitive to paleoenvironmental conditions with clear and

observable indications [13–15]. The sedimentary-diagenetic environment and paleoclimate conditions of sedimentary rock formations can therefore be analyzed on the basis of major and trace elements in sedimentary rocks and changes in their ratios.

The increasing difficulty of shallow oil and gas extraction in China has led to a shift towards deep exploration and development [16,17]. Primary pores in reservoirs with a depth >3000 m are nearly absent owing to strong compaction and cementation [18], and deposits are dominated by secondary pores. However, recent studies [19–22] have shown that primary pores in a clastic reservoir can be preserved under specific geological conditions at about 3500–4500 m and form a high-quality reservoir. The Lenghuqi area is located in the center of the northern margin of the Qaidam Basin. Previous studies have summarized the characteristics and controlling factors of deep reservoirs in detail [23,24] and suggested that the sedimentary environment and deep ultra-high pressure layer are the main controlling factors of deep high-quality clastic reservoirs in the region. Carbonate cement also has a substantial impact on reservoir properties. However, few studies have addressed the paleoclimate conditions and diagenetic environments that existed during the formation of these reservoir rocks. The diagenesis process and diagenetic environment are critical factors required to clarify the evolution process of the reservoir rocks [25]. Further study on the sedimentary-diagenetic environment of the high-quality clastic reservoirs in the Xiaganchaigou Formation of the Oligocene can therefore provide a geological basis for the prediction of high-quality reservoir distribution laws.

2. Geological Setting

The Qaidam Basin located in northwest China is the largest continental basin in the northeastern Tibetan Plateau with a total area of 120,000 km² [26]. The basin has undergone compressional tectonic settings throughout the Cenozoic [26] and is bound by the Eastern Kunlun fault zone to the southwest, the South Qilian fault zone to the northeast, and the Altyn Tagh fault zone to the northwest [27] (Figure 1). The basin developed an exceptionally thick Tertiary sedimentary succession, of which the average thickness is up to 6 km and the maximum thickness is >10 km [28]. The basin is divided into four first-order structural units: the Western Qaidam Basin Uplift, the Yilingping Sag, the Sanhu Sag, and the Northern Qaidam Basin Uplift [29]. The Northern Qaidam Basin Uplift lies in front of the South Qilian Mountains and the Lenghuqi area is located in the center of the uplift.

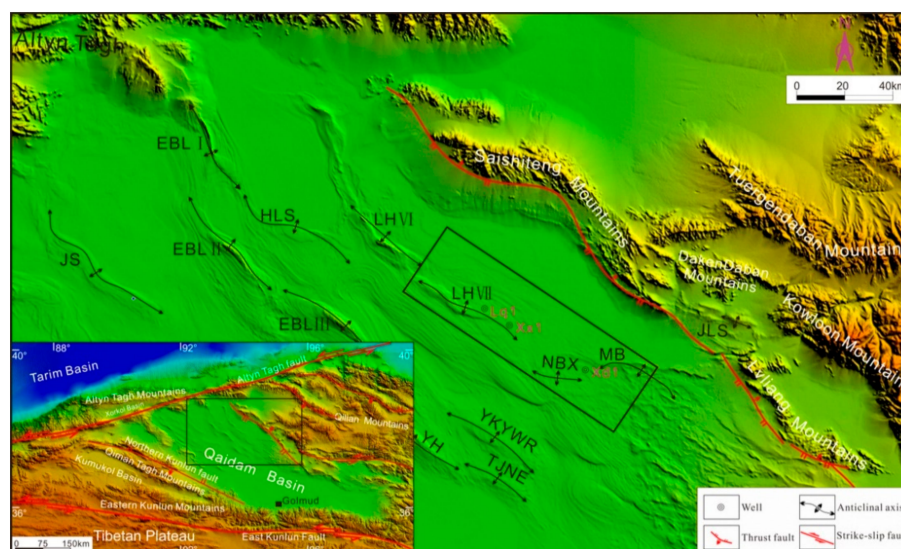


Figure 1. Structural location of the Lenghuqi area in the northern margin of the Qaidam Basin.

The ancient lake basin of the Qaidam Basin underwent three evolution stages from Paleogene to Neogene: the lake basin first appeared in the Paleocene and early Eocene, the paleolake then continuously expanded from late Eocene to Oligocene, and reached its maximum extent in the

subsidence stage of the Oligocene. The paleolake then gradually shrank during the Early Miocene to Pliocene [30,31]. The Paleogene and Neogene strata can be divided into six units on the basis of previous stratigraphic results from the northern Qaidam Basin. These six stratigraphic units (in ascending order) are the Lulehe Formation (E₁₊₂, Paleocene to early Eocene, ~65~45 Ma), Xiaganchaigou Formation (E₃, middle to late Eocene, ~45~35.5 Ma), ShangGanchaigou Formation (N₁, late Eocene to Oligocene, ~35.5~22 Ma), XiaYoushanshan Formation (N₂¹, early to middle Miocene, ~22~15 Ma), ShangYoushanshan Formation (N₂², middle to late Miocene, ~15~8 Ma), and Shizigou Formation (N₂³, late Miocene to Pliocene, ~8~2.8 Ma) [32–35]. In recent years, abundant oil and gas reservoirs in Paleogene strata have been found in the central area of the northern Qaidam Basin, which indicates abundant oil and gas resources in this area [36,37].

3. Materials and Methods

The Xiaganchaigou Formation (E₃) in the Lenghuqi area is deeply buried with an average depth of >4000 m. Samples were collected from drill core of the Xx1 well (Figure 1). The Xx1 well is located at 93°52′41″E, 38°7′34″N. It is 5500 m deep and its wellhead is 2829 m above sea level. One 5.64-m drill core was obtained between 4111.34 and 4117.09 m with a harvest rate of 98.1% (Figure 2a), and another drill core of 8.72 m was obtained between 4847.00 and 4855.82 m with a harvest rate of 98.9% (Figure 2b). The lithology and logging characteristics of the core section of the Xx1 well are shown in Figure 2. Whole rock and clay mineral compositions are listed in Table 1. X-ray diffraction (XRD) was performed following techniques outlined by the Qinghai Oilfield Exploration and Development Research Institute of PetroChina (SY/T5163-2010 X-ray Diffraction Analysis Method for Clay Minerals and Common Non-clay Minerals in Sedimentary Rocks). Twenty-five whole rock and clay mineral components were determined (Table 1). We use the XRD results in combination with microscopic observations, scanning electron microscopy, and electron probe analysis of the rock flakes to identify the clay mineral development characteristics in the Xiaganchaigou Formation from the Oligocene mudstones and sandstones in the Lenghuqi area of the Qaidam Basin.

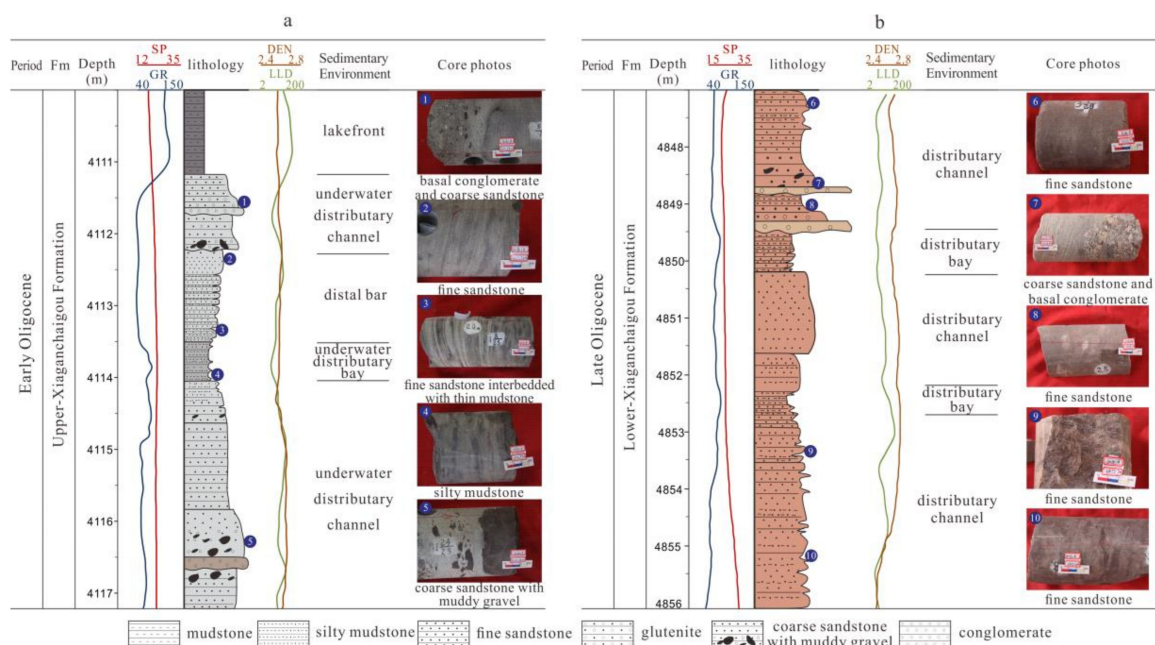


Figure 2. Sedimentological and petrophysical characteristics of the Xx1 well. (a): Upper-Xiaganchaigou Formation; (b): Lower-Xiaganchaigou Formation.

Table 1. X-ray Diffraction Results of Whole Rock and Clay Mineralogy of the Xiaganchaigou Formation.

Buried Depth	Formation	Mineral Type and Content (%)					Total Amount of Clay (%)	Relative Content of Clay Minerals (%)					Mixed Layer Ratio (%)
		Quartz	Potassium Feldspar	Sodium Feldspar	Calcite	Anhydrite		S	I/S	I	K	C	
4111.51	Upper Xia Ganchaigou Fm.	68.2	6	9.4	3.8	/	12.6	/	32	44	/	24	6
4111.75		47.6	6	16.2	20.3	/	9.9	/	19	47	/	34	10
4112.11		47.4	9.5	10.3	11.4	/	21.3	/	11	72	/	17	12
4112.64		69.9	2.2	7.1	7.9	0.8	12.1	/	26	54	/	20	5
4112.99		45.1	3.9	12.1	16.6	/	22.4	/	7	80	/	13	9
4113.65		49.7	9.9	9.9	14.5	/	16.0	/	15	69	/	16	10
4114.16		46.7	9.9	9.9	14.3	1.1	18.1	/	30	61	/	9	10
4114.82		42.8	9.5	17.1	6.4	/	21.8	/	32	42	/	26	12
4115.27		70.2	3.6	8.4	5.2	/	12.7	/	25	58	/	17	8
4115.60		60.7	10.3	14.1	4.1	/	10.8	/	22	51	/	27	5
4115.72		64.7	5.2	11.9	2.9	/	15.4	/	11	62	/	27	7
4116.04		68.1	3.6	10	5.1	/	13.3	/	51	31	/	18	14
4116.34		53.9	14.9	12.6	6.4	/	12.3	/	38	41	/	21	15
Average		56.72	7.27	11.46	9.15	0.16	15.28	/	24.54	54.77	/	20.69	9.46
4847.08	Lower Xia Ganchaigou Fm.	49.1	11.9	20.9	11.5	/	6.6	/	9	84	/	7	11
4849.23		65.6	4.5	11.8	2.1	/	15.9	/	5	72	/	23	12
4850.46		57.7	10.5	23	1.4	/	7.4	/	4	78	/	18	13
4851.00		68.6	5	11.9	2.3	1.5	10.7	/	16	73	/	11	9
4851.39		59.9	17	13.7	1.8	/	7.7	/	24	53	/	23	7
4851.68		54.9	5.5	13	17.6	/	9.2	/	4	64	/	32	10
4852.40		42.6	21.7	7.3	24.2	/	4.1	/	18	69	/	13	13
4853.37		56.7	5.8	7.4	20.1	/	10.0	/	2	80	/	18	10
4853.91		62.5	5.7	12.9	6	/	13.0	/	3	79	/	18	11
4854.38		49	12.5	15.2	6.7	/	16.6	/	11	82	/	7	10
4854.62		59.7	5.5	10.6	7.5	1.5	15.2	/	5	69	/	12	14
4855.30	49	7.3	13.4	14.4	/	15.9	/	6	76	/	13	5	
Average	56.28	9.41	13.43	9.63	0.27	11.03	/	8.92	73.25	/	16.25	10.42	

Standard: SY/T 5163-1995. The reason that $S + I/S + I + K + C + C/S = 101$ or 99 is rounded numbers rather than data bias. The clay mineral with a mixed-layer ratio $> 70\%$ is smectite. S is smectite, I/S is mixed-layer illite/smectite, I is illite, K is kaolinite, and C is chlorite. The mixed layer ratio (e.g., 20%) indicates that the smectite content in the mixed layer illite/smectite is 20%.

Samples were observed microscopically prior to chemical analysis to monitor potential alteration, mineralization, or secondary weathering. All samples were ground with a non-contaminating crusher, screened in a 200-mesh sieve, and heated in an oven at $80\text{ }^{\circ}\text{C}$ for 3 h to remove moisture. Major element measurements were performed using a fluorescence spectrometer 3080E3X (Rishi Electric Corporation, Japan). We used HF + HNO₃ to seal and dissolve samples during trace element analysis using laser coupled plasma mass spectrometry (ICP-MS). Analyses were completed in the Lanzhou Oil and Gas Resources Research Key Laboratory in the Institute of Geology and Geophysics at the Chinese Academy of Sciences.

4. Results

4.1. Clay Minerals

The test results show that illite is the most abundant mineral in all samples, followed by chlorite and the mixed layer illite/smectite. Smectite and kaolinite were not detected. The quartz content in the lower Xiaganchaigou Formation ranges from 42.6% to 68.6% with an average of 56.28%. The clay mineral content ranges from 4.1% to 16.6% with an average of 11.03%. The illite content in the clay minerals ranges from 53% to 84% with an average of 73.25%. The chlorite content ranges from 7% to 23% with an average of 16.25%. The mixed layer illite/smectite content ranges from 6.6% to 16.6% with

an average of 8.92% and average smectite content in the mixed layer illite/smectite of 10.42%. In the Upper Xiaganchaigou Formation, the quartz content ranges from 42.8% to 70.2% with an average of 56.72%. The clay mineral content ranges from 9.9% to 22.4% with an average of 15.28%. The illite content in the clay minerals is substantially lower than that in the lower Xiaganchaigou Formation; ranging from 31% to 80% with an average of 54.77%. The mixed layer illite/smectite content ranges from 7% and 51% with an average of 24.54% with an average smectite content in the mixed layer illite/smectite of 9.46%. The chlorite content is also somewhat higher, ranging from 9% to 34% with an average of 20.69%.

The illite in the upper member sandstone of the Xiaganchaigou Formation is mostly filamentous or bridging between particles (Figure 3a). The mixed layer illite/smectite is more developed, usually on particle surfaces or filled between particles (Figure 3a–d). The illite in the lower member sandstone of the Xiaganchaigou Formation is filled with curved leaves or scales between particles (Figure 3e). The mixed layer illite/smectite is less common, and flaky chlorite is visible on the particle surfaces (Figure 3f).

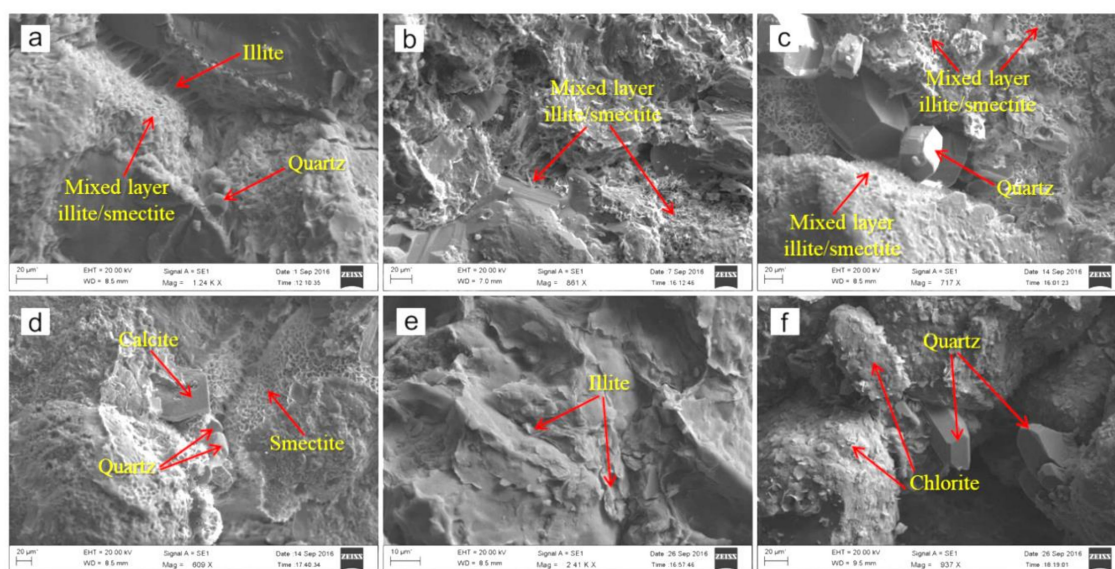


Figure 3. Scanning electron micrograph of sandstone from the Xiaganchaigou Formation (Xx 1 well). (a) 4111.51 m, upper Xiaganchaigou Formation, filamentous illite, mixed layer illite/smectite, and other clay minerals filled between particles and particle surfaces; (b) 4115.37 m, upper Xiaganchaigou Formation, mixed layer illite/smectite filled between particles and particles surfaces; (c) 4209.77 m, upper Xiaganchaigou Formation, interstitial calcite, self-generated and enlarged quartz. Particle surfaces develop a mixed layer illite/smectite clay mineral; (d) 4122.14 m, upper Xiaganchaigou Formation, interstitial calcite. Particle surfaces develop a mixed layer illite/smectite clay mineral; (e) 4850.00 m, lower Xiaganchaigou Formation, curved leaf-like illite clay completely filled in intergranular pores; (f) 4853.05 m, lower Xiaganchaigou Formation, intergranular pores are developed, self-generated and enlarged quartz. Chlorite is developed on the particle surfaces.

The illite content in the lower member is substantially higher than that in the upper member and the mixed layer illite/smectite content also reduces downwards. This indicates that the clay minerals in the sandstone are mainly self-generated. Their combined characteristics reflect their formation conditions, including the climate and sedimentary and diagenetic environments. Kaolinite is mostly distributed in moist tropical or subtropical regions [4,26] and mainly forms from feldspar leaching and weathering [27], as well as weathering and low-temperature hydrothermal metasomatism [28]. In contrast to the kaolinite formation environment, chlorite can only be preserved in areas with weak chemical weathering [1]. Smectite is associated with a warm–humid–cold climate, pervasive within sediments in temperate and semi-humid regions [26], and its contents tend to decrease with warmer

temperatures [29]. Illite mainly forms in dry and cold climates [30,31] and the combination of clay minerals dominated by illite reflects an arid–semi-arid climate [26]. The clay mineral combination of the Xiaganchaigou Formation sandstone in the Lenghuqi area is dominated by the I + I/S + C type, which displays distribution characteristics of high illite content, higher mixed layer illite/smectite and chlorite content, low smectite, and missing kaolinite. This suggests that the sedimentary basin in the Oligocene (i.e., the Xiaganchaigou Formation sedimentary period) was generally in an arid–semi-arid climate with weak leaching and chemical weathering.

Authigenic kaolinite mainly forms by feldspar leaching in an acidic medium followed by the direct formation of pore water during diagenesis [26,32,33]. Kaolinite is therefore an indicator mineral for weakly acidic environments with leaching and strong chemical weathering [28,29]. Authigenic smectite usually forms in alkaline media that is depleted in K^+ but enriched in Na^+ and Ca^{2+} [4,34]. Illite mainly forms by the weathering of potassium feldspar, mica, and other aluminosilicate minerals in a hydrous K^+ -rich alkaline medium under weak leaching [4,26,35,36]. Fe^{2+} and Mg^{2+} in smectite are replaced by Al^{3+} and K^+ during dehydration [32]. Smectite may also form from the precipitation of pore water in an alkaline medium [37]. Chlorite forms by the precipitation of pore water rich in Mg^{2+} in a relatively high-temperature and more strongly-alkaline environment [26]. Illite is more stable in a water environment with a high K^+/H^+ ratio. The presence of the mixed layer illite/smectite reflects the gradual transition of smectite to illite in a K^+ -rich alkaline environment, and chlorite forms in a Mg^{2+} -rich alkaline environment [26,32]. The clay mineralogical characteristics of the Xiaganchaigou Formation sandstone in the Lenghuqi area reflect a diagenetic and primarily alkaline environment rich in K^+ and Mg^{2+} .

4.2. Major Element Analysis

Environmental conditions influence the behavioral characteristics of elements and compounds, including decomposition, migration, and the enrichment of various elements with different properties. A change of sediment chemistry can reflect a change in environmental conditions during deposition. Common major oxides (CaO , MgO , K_2O , Na_2O , SiO_2 , Al_2O_3 , Fe_2O_3 , and TiO_2) are sensitive to paleoenvironmental conditions and have clear environmental indications [9,10]. The major oxide compositions measured from samples from the Lenghuqi area are listed in Table 2. The results (Figure 4) show a clear correlation between the oxides. The overall change of oxide content in the lower Xiaganchaigou Formation is small, and the oxide content in the upper member varies greatly. This indicates that climate change in the lower member was not substantial during the sedimentary period. On the other hand, paleoclimatic change in the upper member occurred relatively frequently during the sedimentary period, and the climate fluctuated considerably.

High $CaCO_3$ levels in a closed or semi-enclosed inland lake during the early stages of chemical deposition represent an arid climate, whereas low $CaCO_3$ levels represent a relatively humid climate [38–40]. Ca^{2+} and Mg^{2+} commonly exchange for one another but the large ionic radius of Ca^{2+} enhances its migration. Thus, an environment enriched in Ca^{2+} was likely drier than an environment enriched in Mg^{2+} [10]. The average CaO and MgO contents from the upper Xiaganchaigou Formation samples are 3.23% and 1.26%, respectively, whereas those of the lower Xiaganchaigou Formation are 6.14% and 0.78%. Compared with the upper Xiaganchaigou Formation, the lower Xiaganchaigou Formation is characterized by high CaO and Na_2O and low K_2O , MgO , and TiO_2 (Figure 5). This supports that the lower Xiaganchaigou Formation formed in a relatively dry climate with strong evaporation, while the upper member formed in a relatively warm and humid environment with less evaporation [41,42]. The change of Ti content and other elements reflects the extent of the addition of terrigenous materials. Higher Ti values are associated with richer terrigenous material contents, indicating a warm and humid climate background [43,44]. The paleoclimate characteristics of the sedimentary period of the Xiaganchaigou Formation therefore gradually became humid from early to late in the deposition sequence.

Table 2. Major oxide contents of the Xiaganchaigou Formation in the Lenghuqi structural belt.

Formation	Buried Depth	Lithology	Na ₂ O (%)	MgO (%)	Al ₂ O ₃ (%)	SiO ₂ (%)	K ₂ O (%)	CaO (%)	TiO (%)	Fe ₂ O ₃ (%)	P ₂ O ₅ (%)	MnO (%)
Upper Xia Ganchaigou Fm.	4111.49	Dark gray medium sandstone	2.15	0.51	7.90	79.75	1.66	1.97	0.09	2.26	0.05	0.12
	4111.64	Dark gray fine sandstone	2.00	0.77	8.88	76.77	1.80	2.47	0.13	3.13	0.05	0.11
	4112.24	Reddish-brown mud-bearing fine sandstone	1.52	2.98	16.69	64.37	4.05	0.54	0.32	5.90	0.13	0.07
	4113.54	Dark gray fine sandstone	2.04	1.05	10.07	68.64	2.03	5.18	0.24	2.96	0.09	0.09
	4114.04	Gray-white mud-bearing medium sandstone	1.93	0.98	9.68	68.78	1.94	6.87	0.26	2.76	0.09	0.13
	4114.50	Gray-white mud-bearing medium sandstone	1.86	1.39	11.99	71.18	2.53	3.15	0.26	3.49	0.10	0.10
	4115.44	Gray-white medium sandstone	2.19	0.44	7.91	80.38	1.76	2.01	0.08	2.05	0.04	0.12
	4116.24	Gray-white coarse sandstone	2.15	0.31	7.08	78.63	1.61	2.31	0.08	1.70	0.04	0.13
	4116.99	Gray-white mud-bearing medium sandstone	1.60	2.87	15.37	57.87	3.46	4.53	0.44	6.25	0.13	0.09
Average			1.94	1.26	10.62	71.82	2.32	3.23	0.21	3.39	0.08	0.11
Lower Xia Ganchaigou Fm.	4847.45	Brown red fine sandstone	1.86	1.12	9.15	67.38	2.49	7.02	0.19	2.55	0.03	0.09
	4847.75	Brown red fine sandstone	2.07	1.22	9.90	73.81	2.54	2.98	0.20	3.30	0.02	0.15
	4848.30	Brown red fine sandstone	1.89	0.84	8.34	68.70	2.29	7.23	0.18	2.47	0.01	0.11
	4849.00	Gray-green medium sandstone	2.15	1.88	10.73	70.86	2.65	2.87	0.20	3.63	0.05	0.13
	4849.50	Brown red fine sandstone	1.88	0.62	7.45	69.66	2.10	7.76	0.13	2.11	0.02	0.12
	4850.00	Brown red fine sandstone	2.40	0.67	8.20	77.81	2.08	2.70	0.14	2.49	0.02	0.14
	4850.30	Brown red fine sandstone	2.63	0.49	8.03	83.31	1.91	0.74	0.12	2.16	0.02	0.12
	4851.00	Brown red fine sandstone	2.04	0.68	7.80	69.97	2.07	7.22	0.16	2.23	0.02	0.10
	4852.00	Gray-brown fine sandstone	3.14	0.29	7.22	83.19	1.81	0.69	0.08	1.90	0.01	0.13
	4852.70	Gray-brown fine sandstone	2.92	0.46	7.37	79.06	1.86	2.48	0.09	1.99	0.01	0.12
	4853.50	Gray-brown fine sandstone	2.02	0.30	6.09	68.05	1.73	9.94	0.10	1.76	0.01	0.13
	4853.90	Brown red fine sandstone	1.20	0.27	5.16	58.51	1.82	15.94	0.09	1.58	0.01	0.10
	4854.30	Brown red fine-silt sandstone	1.64	0.33	6.08	62.06	1.82	12.91	0.13	1.75	0.01	0.10
	4855.00	Brown red fine-silt sandstone	2.12	1.71	9.88	68.59	2.31	5.50	0.21	2.45	0.02	0.09
Average			2.14	0.78	7.96	71.50	2.11	6.14	0.15	2.31	0.02	0.12

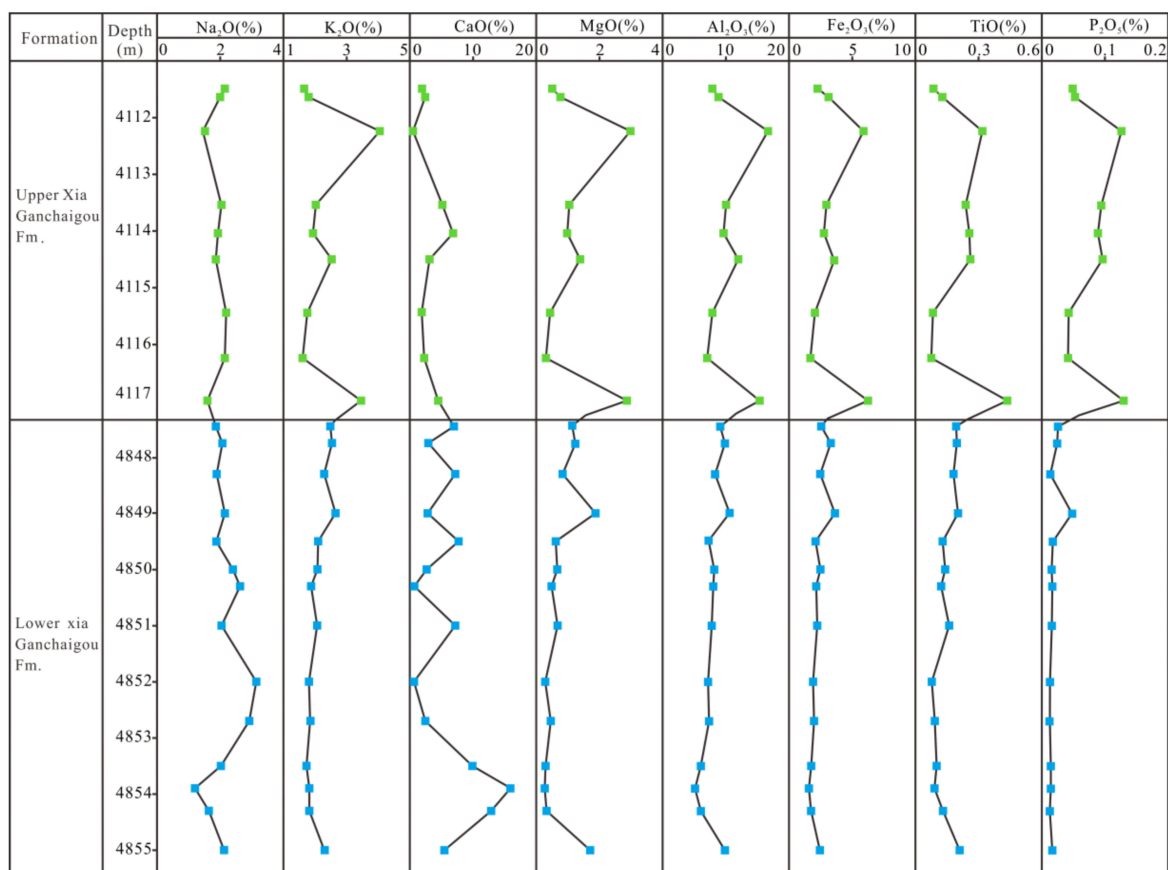


Figure 4. Major oxide content of the Xiaganchaigou Formation in the Lenghuqi structural belt.

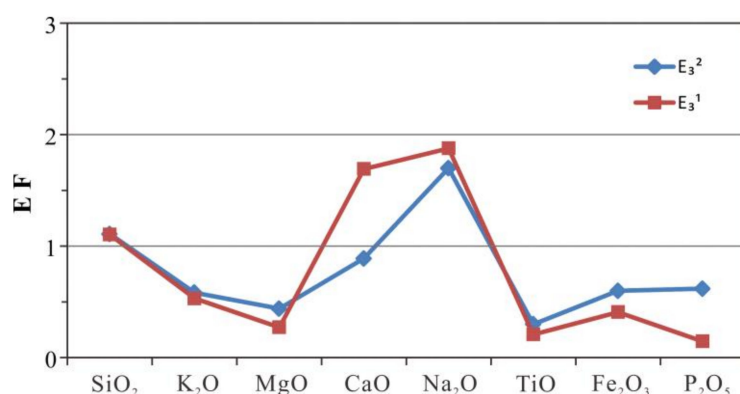


Figure 5. Comparison of major oxides measured in samples and those of the average shale [40]. (EF (enrichment factor) = $C_{\text{sediment}}/C_{\text{standard rock}}$). E_3^2 = Upper Xiaganchaigou Formation. E_3^1 = Lower Xiaganchaigou Formation.

4.3. Trace Element Analysis

The chemical distribution in a rock layer depends on the physical and chemical properties of the elements themselves, which are also substantially affected by paleoclimate and paleoenvironment. The distribution of trace elements and ratio changes are therefore also indicative of the paleoclimate evolution [11,12,14,45,46]. For example, the compositions of Sr, Ba, Ti, Fe, P, Mn, and the Mg/Ca and Sr/Cu ratios are sensitive geochemical indicators and parameters for identifying changes in sedimentary environment [15].

In lacustrine sediments without seawater intrusion, $Sr/Ba > 1$ typically indicates the onset of lake alkalization, whereas $Sr/Ba < 1$ typically indicates freshwater deposition [9,46]. Sr/Cu ratios between 1 and 10 indicate a warm and humid climate, and values > 10 represent arid climatic conditions [15]. The Sr/Ba values of all the samples in the Xiaganchaigou Formation are less than 1 (Table 3) and the average values of the upper and lower members are not substantially different: 0.29 and 0.22, respectively. All Sr/Cu values in the upper Xiaganchaigou Formation aside from one data point are < 10 with an average value of 8.58. All Sr/Ba values in the lower member aside for two data points are > 10 with an average of 14.39. The Ba content in the Xiaganchaigou Formation is significantly higher than that in the average shale [47] (Figure 6). The distribution of Sr/Ba and Sr/Cu demonstrates that the depositional environment of the Xiaganchaigou Formation was mainly dominated by a freshwater sedimentary environment during the sedimentary period. The climate was relatively dry in the early stage and humid in the later stage.

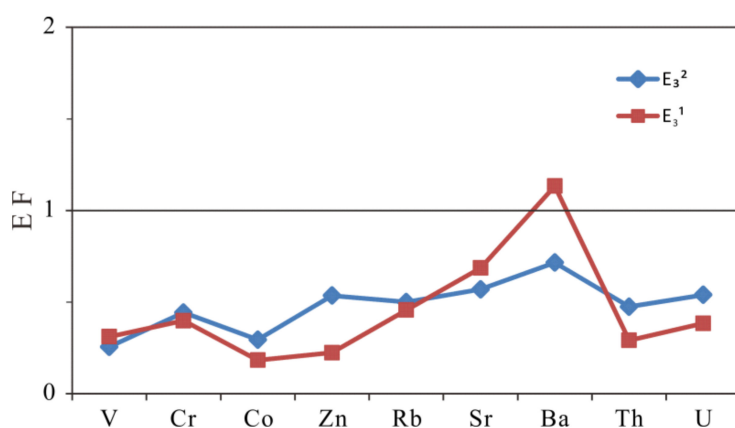


Figure 6. Comparison of trace elements between samples and the average shale. EF (enrichment factor) = $C_{\text{sediment}}/C_{\text{standard rock}}$. E_3^2 = Upper Xiaganchaigou Formation. E_3^1 = Lower Xiaganchaigou Formation.

Table 3. Partial trace element content of the Xiaganchaigou Formation in the Lenghuqi Area.

Formation	Buried Depth	Element Content (mg/kg)										Ratio	
		V	Cr	Co	Ni	Cu	Zn	Sr	Ba	Th	U	Sr/Cu	Sr/Ba
Upper Xia Ganchaigou Fm.	4111.49	23.05	53.46	4.85	8.86	11.54	32.87	132.00	572.10	4.28	0.95	11.43	0.23
	4111.64	40.03	44.72	5.71	11.44	12.94	40.84	108.07	391.96	5.19	1.29	8.35	0.28
	4112.24	86.64	63.00	11.20	29.03	12.66	80.66	117.53	782.20	13.15	3.38	9.28	0.15
	4114.04	38.99	59.30	9.57	15.66	20.08	50.51	131.46	280.50	7.66	1.92	6.55	0.47
	4114.50	48.46	63.18	9.10	16.14	11.60	60.21	114.03	438.07	9.56	2.23	9.83	0.26
	4115.44	18.94	31.56	4.04	8.14	11.00	32.47	97.58	436.59	4.13	0.94	8.87	0.22
	4115.89	36.91	44.32	6.59	11.54	12.64	42.43	115.49	313.19	7.64	1.84	9.14	0.37
	4116.24	14.63	30.37	3.16	7.55	15.26	24.38	95.79	509.03	3.89	0.84	6.28	0.19
	4116.99	97.24	65.08	11.47	27.90	18.56	87.80	139.52	347.24	12.86	3.70	7.52	0.40
Lower Xia Ganchaigou Fm.	4847.45	38.40	43.68	4.88	10.33	9.11	20.60	121.31	469.56	5.27	1.41	13.31	0.26
	4847.75	46.57	61.62	6.52	11.22	12.26	27.12	118.02	718.14	5.66	1.63	9.63	0.16
	4848.30	35.11	45.67	4.34	9.34	9.14	16.69	119.87	427.95	5.32	1.34	13.12	0.28
	4849.00	53.52	58.99	8.97	11.09	15.72	49.91	110.48	400.82	8.60	1.60	7.03	0.28
	4849.50	34.68	32.86	3.73	7.75	9.04	14.26	137.74	819.29	3.64	1.02	15.24	0.17
	4850.00	55.20	47.37	4.21	6.65	10.74	18.27	121.99	611.88	4.16	1.22	11.35	0.20
	4850.30	59.62	48.62	3.48	6.17	8.23	18.23	141.71	859.52	3.58	1.10	17.22	0.16
	4851.00	53.16	46.37	3.69	6.39	8.36	16.91	121.62	429.92	4.34	1.27	14.55	0.28
	4852.00	41.39	41.39	2.83	5.01	8.77	10.13	175.04	1518.69	2.20	0.79	19.96	0.12
	4852.70	51.01	38.82	3.54	5.30	12.06	14.76	206.03	1835.48	2.65	0.88	17.08	0.11
	4853.50	42.24	31.89	2.63	4.28	8.03	14.64	142.31	716.11	2.61	0.91	17.71	0.20
	4853.90	32.35	37.23	2.23	5.03	7.06	12.02	120.66	547.27	3.00	0.82	17.10	0.22
	4854.30	40.76	29.14	2.56	3.44	8.33	8.88	132.45	500.18	3.20	1.02	15.90	0.26
4855.00	70.70	50.93	5.43	10.67	12.36	24.68	152.30	459.19	5.29	1.65	12.32	0.33	

4.4. Rare Earth Elements

Rare earth elements (REE) are a special group of elements that play an important role in geochemistry. Because of the similar chemical nature of the REE, they are typically found together in nature and exhibit only minor differences in their atomic structure. The REE therefore display characteristic fractionation patterns during different geological processes [48].

The REE content of the Xiaganchaigou Formation in the Lenghuqi area is particularly high (Table 4). The distribution of REE contents in the upper member is 52.40–217.73 mg/kg with an average of 117.87 mg/kg. The average concentration of light REE (LREE) is 87.58 mg/kg, accounting for 74.50%, whereas the average heavy REE (HREE) is 30.29 mg/kg, accounting for 25.50%. The distribution of REE in the lower Xiaganchaigou Formation ranges from 33.68 to 98.59 mg/kg with a mean of 75.59 mg/kg. The average LREE is 54.71 mg/kg, accounting for 71.90%, and the average HREE is 20.88 mg/kg, accounting for 28.10%. The normalized REE distribution patterns of in the upper and lower Xiaganchaigou Formation (Figure 7) are similar to those of chondrites [49] and the North American shale [41], which indicates that the sediments have the same material source and formation process [48,50]. The distribution of the total amount of REE (Σ REE) with depth direction is very close to the trend of La, Ce, and Er (Figure 8). The change of Σ REE is closely related to the change of climate and environment, that is, REE content is higher in warm and humid climates and lower in cold and dry climates [51–53]. The REE content of the lower Xiaganchaigou Formation is significantly lower than that of the upper member, indicating that the paleoclimate conditions of sedimentary period in the lower member of the lower Ganchaigou Formation are relatively cold and dry, while the climate in the upper Xiaganchaigou Formation is warmer and humid. This is consistent with the climatic characteristics reflected by clay minerals.

Table 4. Rare earth element content of the Xiaganchaigou Formation in the Lenghuqi Area.

Formation	Buried Depth	Rare Earth Element Content (mg/kg)															
		Sc	Y	La	Ce	Pr	Nd	Sm	Eu	Tb	Gd	Dy	Ho	Er	Tm	Yb	Lu
Upper Xia Ganchaigou Fm.	4111.49	2.56	7.12	11.78	20.84	2.48	9.05	1.68	0.41	0.24	1.49	1.35	0.27	0.77	0.12	0.78	0.12
	4111.64	3.58	9.71	15.21	25.79	3.03	10.97	2.11	0.51	0.30	1.86	1.75	0.35	1.04	0.16	1.05	0.16
	4112.24	13.35	20.86	38.25	69.93	7.89	28.64	4.91	1.01	0.68	4.21	4.05	0.83	2.45	0.38	2.46	0.38
	4114.04	8.47	17.70	23.41	43.86	5.39	20.09	3.82	0.78	0.56	3.48	3.20	0.63	1.81	0.28	1.80	0.28
	4114.50	8.76	15.74	26.29	46.65	5.37	19.46	3.51	0.71	0.50	3.11	2.93	0.60	1.76	0.28	1.81	0.28
	4115.44	2.15	6.98	11.47	20.82	2.45	9.22	1.70	0.42	0.24	1.48	1.37	0.27	0.78	0.12	0.79	0.12
	4115.89	6.74	14.40	21.44	39.09	4.64	17.38	3.31	0.67	0.47	2.95	2.72	0.54	1.58	0.25	1.60	0.25
	4116.24	1.54	6.56	9.34	17.95	2.13	8.14	1.53	0.38	0.23	1.38	1.29	0.26	0.73	0.11	0.73	0.11
	4116.99	12.15	24.85	42.17	74.27	8.48	30.82	5.49	1.09	0.82	4.95	4.87	1.00	2.94	0.46	2.93	0.45
Lower Xia Ganchaigou Fm.	4847.45	4.86	13.11	17.70	31.64	3.94	14.72	2.92	0.69	0.42	2.62	2.39	0.47	1.36	0.21	1.35	0.21
	4847.75	6.46	12.07	15.44	29.87	3.46	13.11	2.57	0.61	0.39	2.36	2.28	0.46	1.32	0.21	1.33	0.21
	4848.30	4.67	11.91	16.02	27.19	3.49	12.95	2.58	0.62	0.37	2.34	2.15	0.43	1.26	0.19	1.24	0.19
	4849.00	6.75	16.24	29.41	56.97	7.24	24.39	4.26	0.89	0.55	3.32	3.18	0.63	1.86	0.30	1.91	0.29
	4849.50	2.85	11.22	12.48	26.60	3.10	12.58	2.66	0.69	0.36	2.45	1.95	0.38	1.03	0.15	0.95	0.14
	4850.00	3.54	10.39	11.60	24.91	2.85	11.66	2.55	0.64	0.36	2.31	2.01	0.39	1.07	0.17	1.04	0.16
	4850.30	2.89	6.25	8.17	17.33	1.86	7.17	1.43	0.40	0.21	1.25	1.22	0.25	0.72	0.11	0.75	0.12
	4851.00	4.14	11.13	13.36	23.17	3.12	11.91	2.31	0.57	0.34	2.08	1.97	0.40	1.17	0.19	1.20	0.18
	4852.00	0.87	4.37	5.13	12.88	1.24	4.65	0.96	0.32	0.15	0.84	0.88	0.18	0.51	0.08	0.52	0.08
	4852.70	2.27	5.35	6.39	13.65	1.57	5.88	1.15	0.40	0.17	1.00	1.02	0.21	0.61	0.10	0.66	0.10
	4853.50	2.51	11.28	10.20	21.02	2.79	11.91	2.67	0.72	0.38	2.47	1.98	0.37	0.99	0.15	0.91	0.13
	4853.90	2.73	8.20	9.05	13.48	2.06	7.54	1.44	0.41	0.22	1.38	1.35	0.28	0.83	0.13	0.84	0.13
	4854.30	2.60	8.16	9.81	15.49	2.34	8.65	1.61	0.43	0.24	1.47	1.43	0.29	0.87	0.14	0.93	0.14
	4855.00	4.44	12.27	15.24	28.99	3.57	13.23	2.59	0.62	0.39	2.32	2.32	0.47	1.40	0.22	1.41	0.22

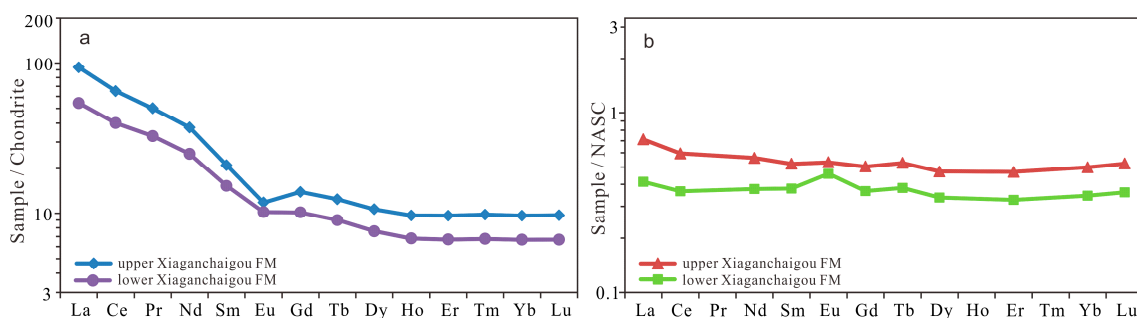


Figure 7. Chondrite-normalized rare earth element (REE) patterns (a) and NASC (North American shale composite)-normalized (REE) patterns (b) of sandstones from the Xiaganchaigou Formation in the Lenghuqi Area. Chondrite data are from [49]; NASC data are from [47].

Formation	Depth (m)	REE(ppm)		La(ppm)		Ce(ppm)		Nd(ppm)		Eu(ppm)		Tb(ppm)		Er(ppm)		
		0	200	400	25	50	50	100	0	20	40	1	20	0,5	10	2
Upper Xia Ganchaigou Fm.	4112															
	4113															
	4114															
	4115															
	4116															
	4117															
Lower xia Ganchaigou Fm.	4848															
	4849															
	4850															
	4851															
	4852															
	4853															
	4854															
	4855															

Figure 8. Rare earth elements contents in the Xiaganchaigou Formation of the Lenghuqi area.

5. Discussion

Sedimentary processes, diagenesis, and weathering may all cause migration and elemental depletion. Sources should therefore be analyzed when using elemental geochemical properties to restore sedimentary environments and paleoclimatic conditions. Only trace elements that are mainly self-generated and maintain their initial content can be used to accurately determine paleoenvironmental conditions [54]. The influence of terrigenous debris on trace element contents can be assessed using the content covariant diagram of Al, Ti, or Th. If the two exhibit a good linear relationship and the Al, Ti, and Th contents are similar to the average shale, the trace elements contained in the sediments or sedimentary rocks are mainly provided by terrigenous debris and therefore not suitable for environmental analysis. Otherwise, it can be used for environmental analysis as reported previously [55–58]. REEs have strong stability during weathering, transport, deposition, and diagenesis, and their solubility in water is very low. The Σ REE in sediments or sedimentary rocks is therefore an indicator of the amount of terrestrial material [59]. The Σ REE of the average shale (PAAS), which is

often used as a standard, is 184.8×10^{-6} . If the ΣREE is close to or higher than this value, the trace elements contained in sediments or sedimentary rocks are mainly provided by terrigenous debris. If the ΣREE in the analyzed sediments or sedimentary rocks is much lower than this value, this shows that it is less affected by terrestrial materials and is mainly authigenic [60,61]. According to the covariant diagram (Figure 9), the correlation between Th and Al, Ti is not very good and the Th, Al, and Ti contents differ significantly from PAAS. The ΣREE content is also substantially lower than the PAAS value, indicating that the REE in the samples are likely mostly authigenic with only a small amount of added terrigenous clastic materials. These data can therefore be used to restore the sedimentary environment and paleoclimate conditions.

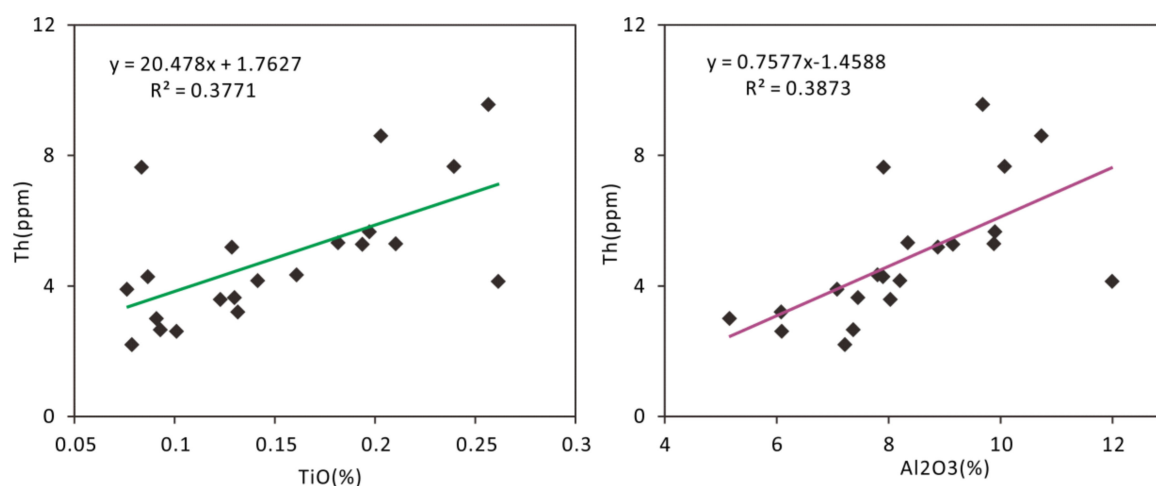


Figure 9. Covariation diagram of Th with Al and Ti from the Xiaganchaigou Formation of the Lenghuqi Area.

Cu and Zn are both transition metal elements. According to the Nernst equation, the pH of the medium environment affects the redox process, and Cu and Zn will partition into the environmental medium with decreasing oxygen fugacity. The redox environment during deposition can therefore be divided according to Cu/Zn. A ratio less than 0.21 represents a reducing environment, between 0.50 and 0.63 represents a weak oxidizing environment, and greater than 0.63 represents an oxidizing environment [62]. The geochemical properties of Th and U vary greatly in an oxidizing environment but are similar in the reducing environment; thus, this feature can be used to interpret the sedimentary environment, where $\&U = U/[0.5 \times (\text{Th}/3 + \text{U})]$. A $\&U$ value greater than one represents a reducing environment and less than 1 represents an oxidizing environment [63]. A Th/U ratio between 0 and two indicates a reducing environment, and the ratio under strongly oxidizing conditions can reach eight [64].

The Cu/Zn values in the samples ranged from 0.32 to 0.94 with a mean value of 0.58, indicating a weakly oxidizing environment. The $\&U$ value is between 0.72 and 1.04 with a mean of 0.93, and the Th/U ratio is between 2.78 and 5.36 with a mean of 3.52, both of which indicate an oxidizing environment. Ce is the only element among the REE with redox properties: it is depleted under oxidizing conditions and enriched in an oxygen-deficient reducing environment. Wright et al. [65] proposed that the sign of $\text{Ce}_{\text{anom}} = \lg [3\text{Ce}_n/(2\text{La}_n + \text{Nd}_n)]$ can be used to assess Ce enrichment. A positive Ce_{anom} value indicates enrichment whereas a negative value indicates a deficit [65], where “n” signifies shale-normalized concentrations using the convention established by Gromet et al. (1984) [41]. The Ce_{anom} values of the samples from the Xiaganchaigou Formation of Lenghuqi ranged from -0.564 to -0.524 , with an average of -0.536 . The samples were therefore depleted in Ce, which mainly reflects an oxidizing environment.

The most important climate warming event since the Cenozoic era occurred from the middle Paleocene to early Eocene when global temperature and sea levels rose rapidly and reached a peak in the early Eocene. A long-term gradual cooling process occurred from the beginning of the middle Eocene to the early Oligocene with global sea levels dropping slowly and permanent ice sheets forming

on the Antarctic continent. It was not until the late Oligocene when the climate warmed again that the permanent ice sheets began to melt [66–70]. During the Eocene-Oligocene transition, studies of sedimentation [71], vegetation changes [72], and animal evolution [73] on the North American continent all show that the climate changed significantly from the late Eocene to early Oligocene, from warm and humid to cold and dry. Studies on the European continent [74,75], Asia, and Oceania [76] also indicate a trend of the Eocene-Oligocene climate becoming colder and drier. This indicates that the global climate entered a dry and cold period during the late Eocene to early Oligocene. The measurements obtained from the Xiaganchaigou Formation (Oligocene) of Lenghuqi also reflect characteristics of a dry and cold global climate during this period. After entering the late Oligocene (as recorded by deposition of the upper Xiaganchaigou Formation), the global climate also entered a brief warming period. Our findings show that the sedimentary environment in the upper Xiaganchaigou Formation was warmer and more humid than the lower member, which reflects the response of this climatic phenomenon.

6. Conclusions

Oligocene strata (the Xiaganchaigou Formation) in the Lenghuqi area of the North Qaidam Basin are deeply buried with an average depth of >4000 m. The illite content in clay minerals is the highest among all phases (73.25%), followed by chlorite (16.25%), and a mixed layer illite/smectite (8.92%). Smectite and kaolinite are not observed in these samples. The average illite, chlorite, mixed layer illite/smectite contents in the upper Xiaganchaigou Formation are 54.77%, 20.69%, and 24.54%, respectively. The combination of clay minerals reflects that the sedimentary basins of the Oligocene (sedimentary period of the Xiaganchaigou Formation) originate from an arid-semi-arid climate with weak leaching and chemical weathering. The diagenetic environment is dominated by a K⁺- and Mg²⁺-rich alkaline environment. Clear characteristics of CaO and Na₂O enrichment with K₂O, MgO, and TiO₂ loss are observed, especially in the lower Xiaganchaigou Formation. The lower member of the Xiaganchaigou Formation shows characteristics of a dry and cold freshwater sedimentary environment with high evaporation, whereas the upper Xiaganchaigou Group is relatively warm and humid with a significantly increased recharge of terrigenous detrital materials. The paleoclimate conditions in the Oligocene period gradually became moister. The variation of Sr, Ba, Cu, Zn, U, Th, and Ce contents and ratios, as well as REE characteristics, suggest that the paleoclimate conditions of the lower Xiaganchaigou Formation during sedimentation were relatively cold and dry, while the climate of the upper Xiaganchaigou Formation became warmer and more humid.

Author Contributions: G.S. conceived the research plan of this study, analyzed the experimental data, and wrote the manuscript. Y.W. collated the experimental data and designed the figures. J.G. conducted the scanning electron microscope image analyses of the sandstones. M.W., Y.J., and S.P. collected data from the Xx 1 well and drew a single well map.

Funding: This work was financially supported by the CAS “Light of West China” Program (Y304RC1SGQ), Nature Science Foundation of Gansu Province (Grant No. 1308RJZA310), and Key Laboratory Project of Gansu Province (Grant No.1309RTSA041).

Acknowledgments: We would like to thank Junli Qiu. for their technical assistance with chemical analyses.

Conflicts of Interest: The authors declare no conflict of interest.

References

1. Xie, Y.; Wang, J.; Li, L.X.; Xie, Z.W.; Deng, G.H.; Li, M.H.; Jiang, X.S. Distribution of the Cretaceous clay minerals in Ordos basin, China and its implication to sedimentary and diagenetic environment. *Geol. Bull. China* **2010**, *29*, 93–104. [[CrossRef](#)]
2. Singer, A. The paleoclimatic interpretation of clay minerals in soils and weathering profiles. *Earth Sci. Rev.* **1980**, *15*, 303–326. [[CrossRef](#)]
3. Deconinck, J.F.; Blanc-Valleron, M.M.; Rouchy, J.M.; Camoin, G.; Badaut-Trauth, D. Palaeoenvironmental and diagenetic control of the mineralogy of Upper Cretaceous Lower Tertiary deposits of the Central Palaeo Andean basin of Bolivia (Potosi area). *Sediment. Geol.* **2000**, *132*, 263–278. [[CrossRef](#)]

4. Tang, Y.J.; Jia, J.Y.; Xie, X.D. Environment significance of clay minerals. *Earth Sci. Front.* **2002**, *9*, 337–341. [[CrossRef](#)]
5. Sun, L.M.; Yang, Y.B.; Wu, Y.X.; Fang, X.F.; Li, L.H.; Li, Y.C.; Zhao, Y.F.; Tian, L.F. Sedimentary environment of Neogene laterite records in the Xihe basin, Inner Mongolia. *Geol. China* **2008**, *35*, 683–690. [[CrossRef](#)]
6. Yu, S.H.; Zheng, H.H. REE of sediments of the Chang Liushui section at Zhong Wei County of Ning Xia and the environmental significance. *Acta Sedimentol. Sin.* **1999**, *17*, 149–155. [[CrossRef](#)]
7. Li, Y.C.; Wang, S.M.; Huang, Y.S. The lake sediments rediments to environmental and climatic change. *Adv. Earth Sci.* **1999**, *14*, 412–416. [[CrossRef](#)]
8. Fan, Y.H.; Qu, H.J.; Wang, H.; Yang, X.C.; Feng, Y.W. The application of trace elements analysis to identifying sedimentary media environment: A case study of Late Triassic strata in the middle part of western Ordos Basin. *Geol. China* **2012**, *39*, 382–389. [[CrossRef](#)]
9. Zhong, W.; Fang, X.M.; Li, J.J.; Zhu, J.J. The Geochemical Record of Paleoclimate during about 7.0 Ma–0.73 Ma in Linxia Basin, Gansu Province. *J. Arid Land Resour. Environ.* **1998**, *12*, 36–43. [[CrossRef](#)]
10. Kuang, S.P.; Xu, Z.; Zhang, S.S.; Ma, Z.D. Applying Geochemistry to Research into Meso-Cenozoic Climate: Discussion on Jurassic Climatic change in Sichuan Basin, China. *J. Qingdao Inst. Chem. Technol.* **2002**, *3*, 4–9. [[CrossRef](#)]
11. Miller, E.K.; Blum, J.D.; Friedland, A.J. Determination of soil exchangeable-cation loss and weathering rates using Sr isotopes. *Nature* **1993**, *362*, 438–441. [[CrossRef](#)]
12. Reinhardt, E.G.; Blenkinsop, J.; Paterson, R.T. Assessment of a Sr isotope ($^{87}\text{Sr}/^{86}\text{Sr}$) vital effect in marine taxa from Lee Stocking Island, Bahamas. *Geo-Mar. Lett.* **1998**, *18*, 241–246. [[CrossRef](#)]
13. Dominik, J.; Stanley, D.J. Boron, beryllium and sulfur in holocene sediments and peats of the Nile delta, Egypt: Their use as indicators of salinity and climate. *Chem. Geol.* **1993**, *104*, 203–216. [[CrossRef](#)]
14. Bailey, S.W.; Hornbeck, J.W.; Priscoll, C.T.; Gaudette, H.E. Calcium inputs and transport in a base poor forest ecosystem as interpreted by Sr isotopes. *Water Resour. Res.* **1996**, *32*, 707–719. [[CrossRef](#)]
15. Liu, G.; Zhou, D.S. Application of microelements analysis in identifying sedimentary environment—Taking Qianjiang formation in the Jianghang Basin as an example. *Pet. Geol. Exp.* **2007**, *29*, 307–311. [[CrossRef](#)]
16. Zhong, D.K.; Zhu, X.M.; Wang, H.J. Analysis on the characteristics and formation mechanism of high quality clastic reservoirs in China. *Sci. China* **2008**, *38*, 11–18. [[CrossRef](#)]
17. Feng, J.R.; Gao, Z.Y.; Cui, J.G.; Zhou, C.M. The exploration status and research advances of deep and ultra-deep clastic reservoirs. *Adv. Earth Sci.* **2016**, *31*, 718–736. [[CrossRef](#)]
18. Schmidt, V.; McDonald, D.A. The role of secondary porosity in the course of sandstone diagenesis. *SEPM Spec. Publ.* **1979**, *26*, 178–207.
19. Taylor, T.R.; Giles, M.R.; Hathon, L.; Diggs, T.N.; Braunsdorf, N.R.; Birbiglia, G.V.; Kittridge, M.G.; Macaulay, C.I.; Espejo, I.S. Sandstone diagenesis and reservoir quality prediction: Models, myths and reality. *AAPG Bull.* **2010**, *94*, 1093–1132. [[CrossRef](#)]
20. Bjørlykke, K.; Jahren, J. Open and closed geochemical systems during diagenesis in sedimentary basins: Constrains on mass transfer during diagenesis and the prediction of porosity in sandstone and carbonate reservoir. *AAPG Bull.* **2013**, *96*, 2193–2214. [[CrossRef](#)]
21. Jin, Z.K.; Su, K.; Su, N.N. Origin of Jurassic deep burial-quality reservoirs in the central Junggar Basin. *Acta Pet. Sin.* **2011**, *32*, 26–31. [[CrossRef](#)]
22. Gao, C.L.; Ji, Y.L.; Gao, Z.Y.; Wang, J.; Ren, Y.; Liu, D.W.; Duan, X.B.; Huan, Z.J.; Cheng, T.R. Multi-factor coupling analysis on property preservation process of deep buried favorable reservoir in hinterland of Junggar Basin. *Acta Sedimentol. Sin.* **2017**, *35*, 577–591. [[CrossRef](#)]
23. Guo, J.J.; Sun, G.Q.; Men, H.J.; Zhu, W.J.; Ma, J.Y.; Zhu, J.; Guan, B.; Shi, J.A. Genetic analysis of anomalously high porosity zones in deeply buried reservoirs in the west part of northern edge of Qaidam Basin, NW China. *Acta Sedimentol. Sin.* **2018**, *36*, 777–786. [[CrossRef](#)]
24. Wang, Y.T.; Sun, G.Q.; Yang, Y.H.; Wang, M.; Ma, F.Q.; Zhang, C.J.; Zhao, J.; Shi, J.A. U-Pb geochronology analysis of detrital zircons in the Paleogene lower Xiaganchaigou formation in the northern Mahai area, northern margin of Qaidam Basin. *J. Lanzhou Univ. Nat. Sci.* **2019**, *55*, 141–149. [[CrossRef](#)]
25. Guo, R.T.; Ma, D.D.; Zhang, Y.S.; Liu, B.; Chen, X.D.; Cui, J.; Wang, P.; Zhang, Q.H.; Jiang, Y.H.; Li, Y.F. Characteristics and formation mechanism of overpressure pore-fracture reservoirs for Upper Member of Xiaganchaigou Formation in the west of Yingxiong ridge, Qaidam Basin. *Acta Pet. Sin.* **2019**, *40*, 411–422. [[CrossRef](#)]

26. Long, H.; Wang, C.H.; Liu, Y.P.; Ma, H.Z. Application of clay minerals in paleoenvironment research. *J. Salt Lake Res.* **2007**, *15*, 21–25. [[CrossRef](#)]
27. Jin, N.; Li, A.C.; Liu, H.Z.; Meng, Q.Y.; Wan, S.M.; Xu, Z.K. Clay minerals in surface sediment of the northwest Parece Vela basin: Distribution and provenance. *Oceanol. Limnol. Sin.* **2007**, *38*, 504–511. [[CrossRef](#)]
28. Wu, B.H.; Yang, H.N.; Li, S.J. *The Mineral Composition of Sediment and Sedimentation of Central Pacific*; Geological Publishing House: Beijing, China, 1993; pp. 44–45.
29. Lu, C.X. Clay minerals as indicators of paleoenvironment. *J. Desert Res.* **1997**, *17*, 456–460.
30. He, L.B. The relation between clay mineral variation of marine sediment cores and paleoclimate. *Chin. Sci. Bull.* **1982**, *27*, 809–812.
31. Yang, Z.S. Mineralogical assemblages and chemical characteristics of clays from sediments of the Huanghe, Changjiang, Zhujiang rivers and their relationship to the climate environment in their sediment source areas. *Oceanol. Limnol. Sin.* **1988**, *19*, 336–346.
32. Fu, W.J. Influence of clay minerals on sandstone reservoir properties. *J. Palaeogeogr.* **2000**, *2*, 59–67. [[CrossRef](#)]
33. Dong, W.H.; Su, X.S.; Hou, G.C.; Lin, X.Y.; Liu, F.T. Study on distribution law of TDS and main ion concentration in groundwater in the Ordos Cretaceous Artesian Basin. *Hydrogeol. Eng. Geol.* **2008**, *35*, 11–16. [[CrossRef](#)]
34. Liu, Y. The clay mineral characteristics and the analysis for sedimentary environment of the Late Cretaceous in Songliao Basin. *Acta Sedimentol. Sin.* **1985**, *3*, 131–137.
35. Yuan, H.R.; Nie, Z.; Liu, J.Y.; Wang, M. Paleogene sedimentary characteristics and their paleoclimatic implications in the Baise Basin, Guangxi. *Acta Geol. Sin.* **2007**, *81*, 1692–1697. [[CrossRef](#)]
36. Hower, J.; Eslinger, E.V.; Hower, M.E.; Perry, E.A. Mechanism of burial metamorphism of argillaceous sediments: I. Mineralogical and chemical evidence. *Geol. Soc. Am. Bull.* **1976**, *87*, 725–737. [[CrossRef](#)]
37. Boles, J.R.; Surdam, R.C. Diagenesis of volcanogenic sediments in a Tertiary saline lake; Wagon Bed Formation, Wyoming. *Am. J. Sci.* **1979**, *279*, 832–853. [[CrossRef](#)]
38. Wang, Y.F. Lacustrine carbonate chemical sedimentation and climatic-environmental evolution—A case study of Qinghai Lake and Daihai Lake. *Oceanol. Limnol. Sin.* **1993**, *24*, 31–35.
39. Xi, X.X.; Mu, D.F.; Fang, X.M.; Li, J.J. Climatic change since the Late Miocene in west China. *Acta Sedimentol. Sin.* **1998**, *16*, 155–160. [[CrossRef](#)]
40. Sun, G.Q.; Yin, J.G.; Zhang, S.C.; Lu, X.C.; Zhang, S.Y.; Shi, J.A. Diagenesis and Sedimentary Environment of Miocene Series in Eboliang III Area. *Environ. Earth Sci.* **2015**, *74*, 5169–5179. [[CrossRef](#)]
41. Gromet, L.P.; Haskin, L.A.; Korotev, R.L.; Dymek, R.F. The “North American shale composite”: Its compilation, major and trace element characteristics. *Geochim. Cosmochim. Acta* **1984**, *48*, 2469–2482. [[CrossRef](#)]
42. Guo, J.J.; Sun, G.Q.; Liu, W.M. Formation phases of carbonate cements and sedimentary environments in lower jurassic sandstones of the lenghu v tectonic belt, north Qaidam basin, China. *Carbonates Evaporites* **2018**. [[CrossRef](#)]
43. Ma, B.L.; Wang, Q. Distribution characteristics of elements in modern sediments of Qinghai lake. *Acta Sedimentol. Sin.* **1997**, *15*, 120–125. [[CrossRef](#)]
44. Yuan, B.Y.; Chen, K.Z.; Bowler, J.M.; Ye, S.J. The formation and evolution of the Qinghai Lake. *Quat. Sci.* **1990**, *10*, 233–243.
45. Wang, S.J.; Huang, X.Z.; Tuo, J.C.; Shao, H.S.; Yan, C.F.; Wang, Q.S.; He, Z.R. Evolutional characteristics and their Paleoclimate significance of trace elements in the Hetaoyuan Formation, Biyang Depression. *Acta Sedimentol. Sin.* **1997**, *15*, 65–70. [[CrossRef](#)]
46. Song, M.S. Sedimentary Environment Geochemistry in the Shasi Section of Southern Rama, Dongying Depression. *J. Mineral. Petrol.* **2005**, *5*, 67–73. [[CrossRef](#)]
47. Taylor, S.R.; McLennan, S.M. *The Continental Crust: Its Composition and Evolution*; Blackwell Scientific Pub.: Palo Alto, CA, USA, 1985; p. 312.
48. Shi, J.A.; Guo, X.L.; Wang, Q.; Yan, N.Z.; Wang, J.X. Geochemistry of REE in QH1 sediments of Qinghai Lake since Late Holocene and its Paleoclimatic significance. *J. Lake Sci.* **2003**, *15*, 28–34. [[CrossRef](#)]
49. McDonough, W.F.; Sun, S.S. The composition of the earth. *Chem. Geol.* **1995**, *120*, 223–253. [[CrossRef](#)]
50. Cao, J.J.; Zhang, X.Y.; Wang, D.; Zhou, J. REE geochemistry of late Cenozoic eolian sediments and the paleoclimate significance. *Mar. Geol. Quat. Geol.* **2001**, *21*, 97–101. [[CrossRef](#)]
51. Kashiwaya, K.; Yamanoto, A.; Fukuyama, K. Time variations of erosional force and grain size in Pleistocene lake sediments. *Quat. Res.* **1985**, *28*, 61–68. [[CrossRef](#)]

52. Zhao, Y.Y.; Wang, J.T.; Qin, C.Y.; Chen, Y.W.; Wang, X.J.; Wu, M.Q. Rare-earth elements in continental shelf sediments of the China Seas. *Acta Sedimentol. Sin.* **1990**, *8*, 37–43. [[CrossRef](#)]
53. Chen, J.A.; Wan, G.J.; Xu, J.Y. Sediment particle sizes and the dry-humid transformation of the regional climate in Erhai Lake. *Acta Sedimentol. Sin.* **2000**, *18*, 341–345. [[CrossRef](#)]
54. Tribouvillard, N.; Algeo, T.J.; Lyons, T.; Riboulleau, A. Trace metals as paleoredox and paleoproductivity proxies: An update. *Chem. Geol.* **2006**, *232*, 32. [[CrossRef](#)]
55. Böning, P.; Brumsack, H.J.; Böttcher, M.E.; Schnetger, B.; Kriete, C.; Kallmeyer, J.; Borchers, S.L. Geochemistry of Peruvian near-surface sediments. *Geochim. Cosmochim. Acta* **2004**, *68*, 4429–4451. [[CrossRef](#)]
56. Calvert, S.E.; Pedersen, T.F. Geochemistry of recent oxic and anoxic sediments: Implications for the geological record. *Mar. Geol.* **1993**, *113*, 67–88. [[CrossRef](#)]
57. Hild, E.; Brumsack, H.J. Major and minor element geochemistry of Lower Aptian sediments from the NW German Basin (core Hoheneggelsen KB 40). *Cretaceous Res.* **1998**, *19*, 615–633. [[CrossRef](#)]
58. Tribouvillard, N.; Desprairies, A.; Lallier-Vergès, E.; Bertrand, P.; Moureau, N.; Ramdani, A.; Ramanampisoa, L. Geochemical study of organic-matter rich cycles from the Kimmeridge Clay Formation of Yorkshire (UK): Productivity vs. anoxia. *Palaeogeogr. Palaeoclimatol. Palaeoecol.* **1994**, *108*, 165–181. [[CrossRef](#)]
59. Murray, R.W.; Brink, M.R.B.T.; Gerlach, D.C.; Russ, G.P.; Jones, D.L. Rare earth, major, and trace element composition of Monterey and DSDP chert and associated host sediment: Assessing the influence of chemical fractionation during diagenesis. *Geochim. Cosmochim. Acta* **1992**, *56*, 2657–2671. [[CrossRef](#)]
60. Chang, H.J.; Chu, X.L.; Feng, L.J.; Huan, J.; Zhang, Q.R. Redox sensitive trace elements as paleoenvironments proxies. *Geol. Rev.* **2009**, *55*, 91–99. [[CrossRef](#)]
61. Nothdurft, L.D.; Webb, G.E.; Kamber, B.S. Rare earth element geochemistry of Late Devonian reefal carbonates, Canning Basin, Western Australia: Confirmation of a seawater REE proxy in ancient limestones. *Geochim. Cosmochim. Acta* **2004**, *68*, 263–283. [[CrossRef](#)]
62. Mei, S.Q. Application of rock chemistry in the study of presinian sedimentary environment and the source of uranium mineralization in Hunan province. *Hunan Geol.* **1988**, *7*, 25–32.
63. Steiner, M.; Wallis, E.; Erdtmann, B.D.; Zhao, Y.L.; Yang, R.D. Submarine-hydrothermal exhalative ore layers in black shales from South China and associated fossils—Insights into a Lower Cambrian facies and bio-evolution. *Palaeogeogr. Palaeoclimatol. Palaeoecol.* **2001**, *169*, 165–191. [[CrossRef](#)]
64. Wignall, P.B.; Twitchett, R.J. Oceanic Anoxia and the End Permian Mass Extinction. *Science* **1996**, *272*, 1155–1158. [[CrossRef](#)] [[PubMed](#)]
65. Wright, J.; Schrader, H.; Holser, W.T. Paleoredox variations in ancient oceans recorded by rare earth elements in fossil apatite. *Geochim. Cosmochim. Acta* **1987**, *51*, 631–644. [[CrossRef](#)]
66. Chang, Y.S.; Zhao, H.; Qin, J.; Li, S.; Zhang, J.P. Sedimentary Response to Paleoclimate Change in the East China Sea Shelf Basin. *Acta Sedimentol. Sin.* **2019**, *37*, 320–329. [[CrossRef](#)]
67. Tuo, S.T.; Liu, Z.F. Global climate event at the Eocene-oligocene transition: From greenhouse to icehouse. *Adv. Earth Sci.* **2003**, *18*, 691–696. [[CrossRef](#)]
68. Zachos, J.; Pagani, M.; Sloan, L.; Thomas, E.; Billups, K. Trends, rhythms, and aberrations in global climate 65 Ma to present. *Science* **2001**, *292*, 686–693. [[CrossRef](#)] [[PubMed](#)]
69. Haq, B.U.; Hardenbol, J.; Vail, P.R. Mesozoic and Cenozoic Chronostratigraphy and Cycles of Sea-Level Change: An Integrated Approach. In *Sea-Level Changes: An Integrated Approach*; Wilgus, C.K., Hastings, B.S., Kendall, C.G.S.C., Posamentier, H.W., Ross, C.A., Van Wagoner, J.C., Eds.; SEPM Special Publication: Broken Arrow, OK, USA, 1988; pp. 71–108. [[CrossRef](#)]
70. Miller, K.G.; Komazin, M.A.; Browning, J.V.; Wright, J.D.; Mountain, G.S.; Katz, M.E.; Sugarman, P.J.; Cramer, B.S.; Christie-Blick, N.; Pekar, S.F. The Phanerozoic record of global sea-level change. *Science* **2005**, *310*, 1293–1298. [[CrossRef](#)]
71. Prothero, D.R. Does climatic change drive mammalian evolution? *GSA Today* **1999**, *9*, 1–7.
72. Wolfe, J.A. Climatic, floristic, and vegetational changes near the Eocene/Oligocene boundary in North America. In *Eocene-Oligocene Climatic and Biotic Evolution*; Prothero, D.R., Berggren, W.A., Eds.; Princeton University Press: Princeton, NJ, USA, 1992; pp. 421–436.
73. Ivany, L.C.; Patterson, W.P.; Lohmann, K.C. Cooler winters as a possible cause of mass extinctions at the Eocene/Oligocene boundary. *Nature* **2000**, *407*, 887–890. [[CrossRef](#)]

74. Cavagnetto, C.; Anddon, P. Preliminary palynological data on floristic and climatic changes during the Middle Eocene-Early Oligocene of the eastern Ebro Basin, northeast Spain. *Rev. Palaeobot. Palynol.* **1996**, *92*, 281–305. [[CrossRef](#)]
75. Blondel, C. The Eocene-Oligocene ungulates from western Europe and their environment. *Palaeogeogr. Palaeoclimatol. Palaeocol.* **2001**, *168*, 125–139. [[CrossRef](#)]
76. Buenhy, N.; Carlson, S.J.; Spero, H.J.; Lee, D.E. Evidence for the Early Oligocene formation of a proto-Subtropical Convergence from oxygen isotope records of New Zealand Paleogene brachiopods. *Palaeogeogr. Palaeoclimatol. Palaeocol.* **1998**, *138*, 43–68. [[CrossRef](#)]



© 2019 by the authors. Licensee MDPI, Basel, Switzerland. This article is an open access article distributed under the terms and conditions of the Creative Commons Attribution (CC BY) license (<http://creativecommons.org/licenses/by/4.0/>).